THE JOURNAL OF PHYSICAL CHEMISTRY B

Article

Cite This: J. Phys. Chem. B 2019, 123, 7740−7747

pubs.acs.org/JPCB

# From a Liquid to a Crystal without Going through a First-Order Phase Transition: Determining the Free Energy of Melting with Glassy Intermediates

Lin Zhuang,[†] Rui Wang,[‡] Gerrick E. Lindberg,[∥] Hongyi Hu,[§] Xin-Zheng Li,[†,⊥] and Feng Wang*[,§]

[†]State Key Laboratory for Artificial Microstructure and Mesoscopic Physics, and School of Physics, Peking University, Beijing 100871, People's Republic of China

[‡]International Center for Quantum Materials, School of Physics, Peking University, Beijing 100871, People's Republic of China

[§]Department of Chemistry and Biochemistry, University of Arkansas, 119 Chemistry Building, Fayetteville, Arkansas 72701, United States

[∥]Department of Chemistry and Biochemistry, and Department of Applied Physics and Materials Science, Northern Arizona University, 700 South Osborne Drive, Flagstaff, Arizona 86011, United States

[⊥]Collaborative Innovation Center of Quantum Matter, Peking University, Beijing 100871, People's Republic of China

Supporting Information

**ABSTRACT:** The excess free energy of a liquid relative to an Einstein crystal reference state is calculated without going through a first-order phase transition. This is accomplished by going through an arrested glassy state to avoid a direct liquid to gas or liquid to crystal transition. The method is demonstrated by calculating the free energy difference between liquid water and ice Ih using the TIP4P and WAIL water models. TIP4P ice Ih melts at 232 ± 1 K, in close agreement with other estimates in the literature. WAIL ice melts at 272 ± 1 K, in good agreement with that of real water, which serves as a good validation of the quality of the WAIL model. The glassy intermediate method is easy to implement and amicable to parallel executions. We expect this method to have broad applications for calculating the liquid excess free energies for other materials.

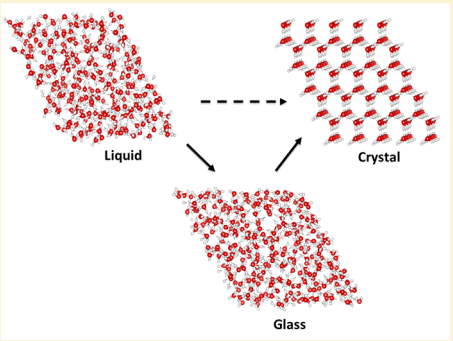


## 1. INTRODUCTION

Computational investigation of the phase diagram is of great significance. Many phase transitions occur under extreme conditions, such as high temperature and pressure or even negative pressure.[1,2] Methods developed for computing phase transitions are thus very helpful for accessing these challenging conditions computationally.[3−5]

Accurate modeling of phase behavior requires both a robust free energy method and an accurate interaction potential. A good model potential should not only provide a high-fidelity description of the potential energy surface, but it also has to be efficient enough to allow for long simulations typically needed for free energy calculations. Proper description of phase transitions is frequently considered an important validation for the quality of a model potential.[6] Advances in free energy determination techniques would thus benefit potential validations. This is especially important for more expensive variants of model potentials, such as polarizable force fields.[7]

One method for measuring free energies is to integrate along a switching variable $\lambda$

$$\Delta A = \int_0^1 \left\langle \frac{\partial H(\lambda)}{\partial \lambda} \right\rangle \mathrm{d}\lambda \tag{1}$$

where $H(1)$ is the Hamiltonian of the system of interest and $H(0)$ is the Hamiltonian of a reference system with a known free energy. $\Delta A$ from eq 1 is generally referred to as the excess free energy relative to the reference system. In practice, many methods exist to perform the integration in eq 1. Although the most straightforward method is probably thermodynamic integration (TI),[8−10] other methods, such as Bennett's acceptance ratio[11] or nonequilibrium integration,[12,13] are also widely used.

For a solid phase, natural choices for the reference system include the Einstein crystal[8,9,14] or the Debye crystal.[15,16] The Debye crystal is a harmonic crystal at the minimum-energy conformation of the solid lattice, and the Einstein crystal is simply a collection of harmonic oscillators that are not interacting with each other.[8,9,14] While several techniques have been proposed to improve the efficiency of the Einstein crystal or Debye crystal based approaches,[16−21] increasing convergence speed and making them suitable for flexible molecules, these approaches are generally not applicable for determining the free energy of a fluid.

Received: July 18, 2019
Revised: August 22, 2019
Published: August 22, 2019







DOI: 10.1021/acs.jpcb.9b06840
J. Phys. Chem. B 2019, 123, 7740−7747

The free energy of a fluid can be determined with the Widom particle insertion method,[22,23] the Gibbs ensemble method,[24] etc.[25] Improved variants of these methods are also available, such as the overlapping distribution approach, devised to improve efficiency for dense liquids.[26,27] However, such fluid-oriented methods generally do not perform well for crystals because the annihilation of a particle in a crystal leads to a defect with a long lifetime.

This situation leads to the frequent use of different approaches and reference states for measuring the free energies of the two states involved in the melting process. For example, using an Einstein crystal as reference for both solids and liquids is challenging because the integration of eq 1 from liquid to the Einstein crystal will require sampling through a first-order phase transition with no overlap of conformation space.

We note that even the integration of eq 1 from a liquid to an ideal gas reference state is challenging. Such a procedure will also involve integrating over a first-order phase transition. One way to avoid such a phase transition is to take advantage of the gas−liquid critical point.[23] By gradually increasing the pressure of a liquid at a constant temperature, the free energy difference between the liquid phase and the supercritical fluid phase can be obtained by integrating $V = (\partial G/\partial P)_T$. The supercritical fluid can then be heated up and converted back into a gas above the critical point to avoid going directly through the phase boundary.[23] This is a fairly long thermodynamic path that requires prior knowledge of the critical point of the model potential.

In this paper, we demonstrate a procedure that can convert a liquid into an Einstein crystal without a first-order phase transition, thus allowing identical reference states to be used for both the solid and the liquid. The determination of the excess free energy is challenging for strongly interacting systems, such as water. The use of the same reference state should lead to better cancelation of dissipative work from the solid and liquid pathways, thus improving the reliability of the melting free energy determined.

With our thermodynamic path, the liquid is first converted into a glass[28] and then from the glass to an Einstein crystal. Due to the similarity between liquid and vitrified glass, the configuration space overlap is expected to be significantly greater than an ideal gas reference state for the liquid. Both vitrification of a liquid and the conversion from glass to Einstein crystal are very straightforward and easy to converge.

The thermodynamics of glass warrant additional discussions. Glass is an out-of-equilibrium state with very slow relaxations. The relaxation time of glass is typically considered to be on the 100 s scale,[1] which is at least 8 orders of magnitude longer than typical simulation lengths. Albeit slow, given infinite time, a glass should eventually reach equilibrium and fall into the free energy basin of the crystal. In this sense, the free energy of an arrested glassy state is not well-defined. These concerns are avoided for the glassy intermediate method by defining the "free energy" of each glassy intermediate based only on the accessible phase space of that intermediate on the simulation time scale. In this case, each realization of the vitrification will result in a different glassy intermediate with an associated "free energy". Such a free energy is not the free energy of the entire glass ensemble. This unconventional definition of free energy will not affect the final excess free energy determination because the glassy conformation is only an intermediate step in the thermodynamic path connecting the liquid to the Einstein crystal. The so-called "free energy" of this intermediate cancels in the evaluation of the free energy difference between the two terminal states. Because each realization of the liquid to Einstein crystal transformation goes through a different glassy intermediate, only the sum of the work values in all of the steps of this transformation should be used for further analysis.

Our glassy intermediate path for determining liquid excess free energy is philosophically similar to an approach by Schmid and Schilling,[29,30] where the free energy for a disordered hard sphere was determined with the help of a wall potential that constrains the conformation space to prevent free diffusion. However, the wall potential requires several parameters and has no analytical gradients outside of the wall. The latter limits its application to Monte Carlo based sampling. Our method is more intuitive, requires fewer parameters, and can be easily implemented in molecular dynamics for more complex systems.

In this paper, we first present a validation of the glassy intermediate protocol by calculating the melting temperature ($T_M$) of ice Ih as described by the TIP4P water model. The $T_M$ of TIP4P ice Ih has been studied extensively.[16,23,31−40] The choice of this model allows the prediction of our method to be compared with published values. We then use this method to calculate the $T_M$ of the Water potential from Adaptive force matching[41−44] for Ice and Liquid (WAIL) potential.[40] The WAIL parameters have been reported previously with an estimated $T_M$.[40] This work provides another estimate of the $T_M$ of the WAIL model along with an independent validation using the direct coexistence method.[34,45−47]

Details of the glassy intermediate free energy protocol are reported in section 2. Simulation parameters are summarized in section 3. The $T_M$ values of TIP4P and WAIL ice Ih are reported in section 4. Finally, a summary and additional discussion are provided in section 5.

## 2. PROTOCOL FOR DETERMINING THE FREE ENERGY OF MELTING

The free energy difference between an arbitrary state and a reference state can be measured by many methods, including TI,[10] free energy perturbation,[48] nonequilibrium integration techniques,[12] and others.[49−52] Although the rates of convergence of these methods differ, the ideas behind these methods are similar. In every case, the system has to sample a series of intermediate points between the two terminal states. Care must be taken to maximize configuration space overlap between these intermediate state points. A first-order phase transition is associated with a sudden change of the dominate configurations; thus, integration of eq 1 through a first-order phase transition is challenging.

In this paper, we determine the $T_M$ of ice Ih by measuring the difference of the excess free energies of the solid and liquid phases relative to the Einstein crystal. We use the nonequilibrium switching method[12,13] to integrate eq 1, but any other integration method would work. We chose the nonequilibrium switching method because it has been implemented in our in-house version of DLPOLY.[53−55] The strong overlap of conformation space for all steps in this approach should facilitate faster convergence for any free energy determination methods.

Our protocol is illustrated schematically in Figure 1. In our protocol, the solid phase is converted to the Einstein crystal by first turning on harmonic tethering with force constant $k$ (step S1). The instantaneous conformation of the nontethered solid is used as the tethering point. The electrostatic interactions are


DOI: 10.1021/acs.jpcb.9b06840
J. Phys. Chem. B 2019, 123, 7740−7747

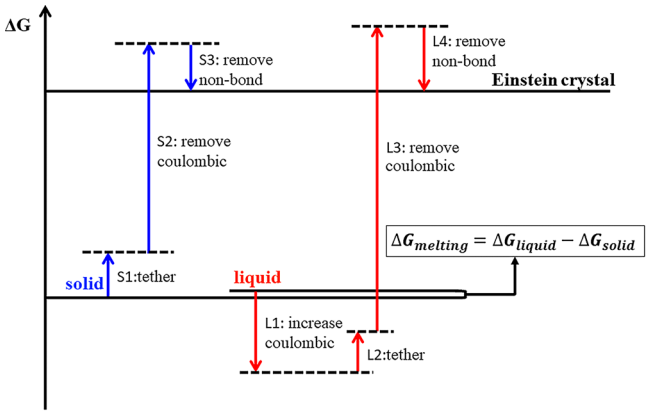


**Figure 1.** Thermodynamics steps used for melting free energy determination.

then removed from the tethered solid in the second step (step S2). Finally, other nonbonded interactions, such as Lennard-Jones (LJ), are removed in the final step (step S3). The harmonic tethering is applied before the removal of intermolecular interactions to avoid vaporization. The excess free energy of the solid is the negative of the sum of the free energies according the equation

$$\Delta G_{\text{solid}} = -(\Delta G_{\text{S1}} + \Delta G_{\text{S2}} + \Delta G_{\text{S2}}) \quad (2)$$

When compared to the solid, determining the excess free energy of the liquid is more challenging. Tethering liquid molecules directly to form a crystal will cause a first-order phase transition. One way to avoid such a transition is to strengthen the intermolecular interactions before introducing the tethering potential. Strengthening the overall intermolecular interaction is equivalent to lowering the temperature. This can be understood by considering that the Boltzmann factor depends on only the ratio of total energy and temperature. Consequently, the liquid will be converted into a glass when intermolecular interactions are strengthened. In the glassy intermediate protocol, rather than strengthening the overall intermolecular interactions, we increase only electrostatic interactions in the first step (step L1). Increasing electrostatic interactions alone is sufficient to cause liquid water to vitrify.

We note that the rate at which liquid is vitrified in step L1 may result in glasses at different stages of aging. However, this would not cause a problem, because the "free energy" of the intermediate state is canceled out when the terminal state free energy difference is calculated. The path is insensitive to the rate of vitrification, and a relatively high vitrification rate can be used. The only requirement for the intermediate states is that the water molecules should be sufficiently vitrified so that they no longer diffuse appreciably when the tethering potentials are applied.

From a glassy immediate state, tethering is applied in a similar fashion to the tethering of the Einstein crystal. This is followed by the removal of electrostatic and nonbonded interactions. We will refer to these steps as step L2, applying tethering restraint; step L3, removing electrostatics; and step L4, removing other nonbonded interactions.

In our work, the same tethering force constant is used in steps S1 and L2. If different force constants are used, the free energy difference between these Einstein crystals will be $\Delta G_{\text{Ein}} = RT \ln\left(\frac{k_t^s}{k_t^l}\right)$ where $k_t^s$ and $k_t^l$ are the tethering force constants for the solid and liquid phases, respectively, and $R$ is the ideal gas constant.

We note that each glassy intermediate configuration has a different set of tethering points. In addition, these tethering points will be different from those of tethered ice Ih. The glassy and ice configurations will also have different densities. These issues are not of concern because the free energy of an Einstein crystal is a function of neither the locations of the tethering points nor the density. This is easily understood because particles in an Einstein crystal do not interact with each other and the accessible volume of each harmonic oscillator is determined only by its force constant.

The nonequilibrium work associated with the realization of each liquid free energy measurement is calculated by

$$W_{\text{liquid}} = (W_{\text{L1}} + W_{\text{L2}} + W_{\text{L3}} + W_{\text{L4}}) \quad (3)$$

The liquid free energy is calculated using the total work in eq 3 as

$$\Delta G_{\text{liquid}} = -RT \cdot \ln(\langle e^{-W_{\text{liquid}}/RT} \rangle) \quad (4)$$

where $\langle \cdot \rangle$ indicates an average over the repetitions.

Finally, the free energy of melting is calculated as

$$\Delta G_{\text{melting}} = \Delta G_{\text{liquid}} - \Delta G_{\text{solid}} + \Delta G_{\text{Ein}} \quad (5)$$

where $\Delta G_{\text{Ein}}$ is zero in this work because the tethering force constant is the same for the solid and liquid branches of the cycle.

It is worth commenting that once the tether points are determined in step S1 for the solid and step L2 for the liquid all subsequent calculations can be run in parallel. Obviously, the solid and liquid free energy computations can be performed independently.

A question remains as to the choice of the optimal force constant for tethering. Generally, a relatively small force constant will lead to a smaller free energy associated with tethering, so that the tethering steps S1 and L2 will be easier to converge. In practice, difficulty arises with potentials that have a very repulsive van der Waals core, for example, TIP4P. If the molecules are allowed to oscillate around the tethering point too much, the removal of short-range repulsion in steps S3 and L4 becomes numerically challenging. This problem has been discussed in the literature, with one possible solution being the use of a soft-core potential[56] for the removal of LJ interactions. Rather than implementing the soft-core potential, a simpler approach is to use larger tethering constants. A stronger tethering potential will restrict the conformation space accessible to the molecule during the removal of the repulsive potential. Consequently, the need to sample the highly numerically challenging part of the LJ potential is eliminated, allowing stable convergence of steps S3 and L4.

## 3. SIMULATION DETAILS

In our study, the initial solid phase was created following the electrostatic switching procedure published previously to sample different proton orientations of ice.[57] The electrostatic switching method creates proton disordered ice Ih configurations with the correct ensemble weight. For the TIP4P model, all of the simulations were performed with a 1 fs time step. For the WAIL simulations, a time step of 0.5 fs was used. For both ice Ih and liquid water simulations, parallelepiped boxes containing 300 water molecules were used with three-dimensional periodic boundary conditions. The ice Ih box was



DOI: 10.1021/acs.jpcb.9b06840
J. Phys. Chem. B 2019, 123, 7740−7747

constructed by stacking the four water molecule unit cell of ice Ih (Figure 2) five times along the *a* and *b* lattice directions and

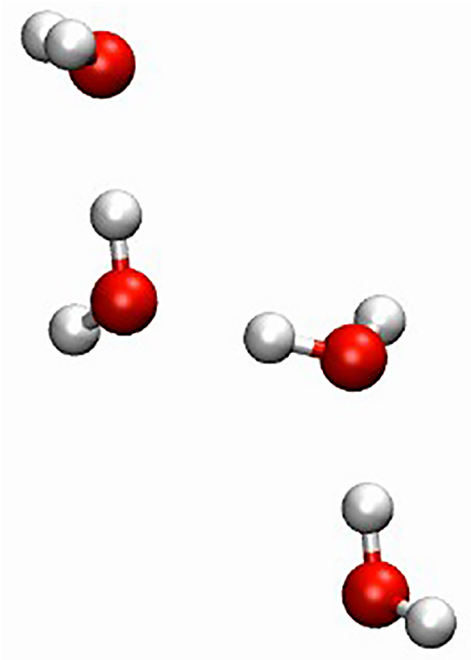

**Figure 2.** Ice Ih unit cell containing four water molecules. The hydrogen atoms are shown in one of the many possible arrangements.

three times along the *c* lattice direction. Such a box size is similar to those used in the literature.[16,58,59] For the WAIL potential, a Nosé−Hoover thermostat with a relaxation constant of 0.2 ps was used for steps S1, S2, L1, L2, and L3. The Nosé−Hoover chain thermostat[60] with a chain length of four also with a 0.2 ps relaxation constant was coupled to each degree of freedom for steps S3 and L4. The Nosé−Hoover chains[60] were used to avoid a previously discussed sampling problem for weakly coupled systems.[57] For the TIP4P potential, a Nosé−Hoover thermostat with a relaxation constant of 0.2 ps was used for every step. Long-range electrostatics were modeled with the particle mesh Ewald method.[54,61] Simulations were performed with a modified version of the DLPOLY version 2.16 program.

The TIP4P densities were determined at each temperature from a 10 ns simulation performed in the constant number of particles, stress tensor, and temperature (*NST*) ensemble for the solid. For the liquid, the corresponding simulations were performed in the constant number of particles, pressure, and temperature (*NPT*) ensemble. The temperature and stress tensor were controlled in this density determination step with the Melchionna modification of the Hoover algorithm[62] with a thermostat relaxation constant of 2 ps and a barostat relaxation constant of 10 ps. The TIP4P ice and water densities were found to be in good agreement with those from prior studies of Vega and co-workers.[63] When determining the melting temperature for the WAIL potential, the experimental density at each temperature for ice Ih and liquid water was used. The densities used for TIP4P and WAIL are summarized in Table 1.

For TIP4P, the melting free energies were measured at five temperatures in the range from 220 to 240 K, and for WAIL, the melting free energies were measured at three temperatures in the range from 253 to 293 K. To avoid sampling problems

**Table 1. Densities Used at Each Temperature for Ice Ih and Liquid Water**

| | | density (g/mL) | |
|---|---|---|---|
| *T* (K) | water model | ice Ih | liquid |
| 220 | TIP4P | 0.943 | 0.996 |
| 225 | TIP4P | 0.940 | 1.006 |
| 230 | TIP4P | 0.941 | 1.001 |
| 235 | TIP4P | 0.940 | 1.005 |
| 240 | TIP4P | 0.939 | 1.006 |
| 253 | WAIL | 0.921 | 0.993 |
| 273 | WAIL | 0.917 | 0.998 |
| 293 | WAIL | 0.917 | 0.998 |

with the repulsive region of the intermolecular potential, the force constant was chosen so that a thermal energy of $k_BT$ would lead to a $(0.1\ \text{Å})^2$ variance for the position distribution around the tethering point. A tethering potential was applied to each atom of a water molecule; thus, that tethered water would not rotate freely. This significantly reduced the rotational entropy of water, thus facilitating convergence.

**Table 2. Force Constant Used at Each Temperature for Ice Ih and Liquid Water**

| | | force constant (kcal/(mol·Å$^2$)) | |
|---|---|---|---|
| *T* (K) | water model | ice Ih | liquid |
| 220 | TIP4P | 174.783 | 174.783 |
| 225 | TIP4P | 178.756 | 178.756 |
| 230 | TIP4P | 182.728 | 182.728 |
| 235 | TIP4P | 186.701 | 186.701 |
| 240 | TIP4P | 190.673 | 190.673 |
| 253 | WAIL | 100.500 | 100.500 |
| 273 | WAIL | 108.445 | 108.445 |
| 293 | WAIL | 116.390 | 116.390 |

The actual force constants used are summarized in Table 2. In steps S1 and L2, tethering was switched on according to the formula

$$H(\lambda) = \frac{1}{2}k_t\cdot\lambda\cdot\sum(\vec{r} - \vec{r}_0)^2 \tag{6}$$

where $\vec{r}_0$ are the tether points, $k_t$is the tethering force constant, and the sum is over all of the tethered atoms. Due to the use of a large tethering force constant, tethering was turned on gradually in three steps for the TIP4P and WAIL potentials with a duration of 5 or 1 ns for each step, respectively.

In steps S2, L1, and L3, electrostatics are switched according to the formula

$$H_{\text{elec}}(\lambda) = \lambda\frac{1}{4\pi\varepsilon_0}\sum\frac{q_iq_j}{r_{ij}} \tag{7}$$

where the sum is taken over all intermolecular charge pairs with Ewald.[64] For switching on electrostatics, this procedure is found to give similar performance when compared to the optimal switching function approach.[65] In step L1, $\lambda$ is increased from 1 to 1.32 in 3 ns for the TIP4P potential and from 1 to 1.21 in 2 ns for the WAIL potential. The values 1.32 and 1.21 correspond to enhancing each individual charge by 15 and 10%, respectively. The $\lambda$ range was chosen so that both



DOI: 10.1021/acs.jpcb.9b06840
J. Phys. Chem. B 2019, 123, 7740−7747

**Table 3. Simulation Time for the TIP4P and WAIL Model at Each Step[a]**

| | | step | | | | | | |
|---|---|---|---|---|---|---|---|---|
| liquid | model | L1 | L2.1 | L2.2 | L2.3 | L3.1 | L3.2 | L4 |
| description | | vitrification | apply 1% of $k_t$ | apply 10% of $k_t$ | apply 100% of $k_t$ | restore electrostatics to the model value | remove electrostatics | remove other nonbonded interactions |
| simulation (ns) | TIP4P | 3 | 5 | 5 | 5 | 3 | 5 | 2.5 |
| | WAIL | 2 | 1 | 1 | 1 | 5 | 5 | 2 |

| solid | model | S1.1 | S1.2 | S1.3 | S2 | S3 |
|---|---|---|---|---|---|---|
| description | | apply 1% of $k_t$ | apply 10% of $k_t$ | apply 100% of $k_t$ | remove electrostatics | remove other nonbonded interactions |
| simulation (ns) | TIP4P | 5 | 5 | 5 | 5 | 2.5 |
| | WAIL | 1 | 1 | 1 | 5 | 2 |

[a] $k_t$ is the tethering force constant.

water models were fully vitrified at the highest temperature simulated. In this work, the mean-square displacement of water is required to be less than 1 Å$^2$/ns to be considered vitrified.

In steps S2 and L3, $\lambda$ is decreased to 0 in 8 ns for the TIP4P model and in 5 ns for the WAIL model. In steps S3 and L4, the short-range non-Coulombic interactions are switched off in 2.5 ns for the TIP4P model and in 2 ns for the WAIL model according to the formula

$$H_{sr}(\lambda) = \lambda \cdot U_{sr} \tag{8}$$

where $U_{sr}$ is the oxygen−oxygen LJ interactions for the TIP4P potential and the Buckingham and short-range hydrogen bond[40,42] interactions for the WAIL potential. Although it is possible to remove electrostatics and nonbonded interactions simultaneously,[66] we did not follow such an approach because it is straightforward to run both steps in parallel. For steps S3 and L4, the system was equilibrated in the starting conformation for 0.5 ns before switching was initiated. The simulation times used at every step for the TIP4P and WAIL are summarized in Table 3.

We note that vitrification in step L1 is competing with crystallization. For the formation of water ice, fortunately spontaneous crystallization is prohibitively slow on a molecular scale. Thus, any vitrification rate that can be practically used in this step should work. For materials where crystallization is quick even on the simulation time scale, one may have to find a vitrification path that suppresses crystallization. For example, for LJ particles, one may have to increase the particle size parameter $\sigma$ only on a fraction of the particles to cause vitrification. It is known that binary mixtures of LJ particles do not crystallize easily and are thus good glass formers.[67]

Also, care has to be taken because excessive diffusion in step L2 could lead to numerical challenges. Thus, liquid has to be sufficiently vitrified in step L1 to ensure insensitivity to the tethering time scale in step L2. As mentioned previously, we require a mean-square displacement of no more than 1 Å$^2$ for each nanosecond. In this case, tethering should be applied over a duration of several nanoseconds. In the Supporting Information, we determined the melting free energy by doubling the vitrification time (L1) from 3 to 6 ns and reducing the tethering time in the liquid tethering steps from 5 to 3 ns. The modified protocol leads to a melting temperature of 230 K, which is within our estimated error bar of $T_M$. Thus, our glassy intermediate protocol is stable with respect to a wide range of rational choices of switching speeds.

## 4. DETERMINATION OF THE MELTING TEMPERATURE OF ICE IH

Table 4 reports the excess free energies for the liquid and solid phases. The free energy estimates were calculated with

**Table 4. Excess Free Energies for the Ice Ih and Liquid Water, Reported in kcal/mol**

| | | $\Delta G$ (kcal/mol) | |
|---|---|---|---|
| $T$ (K) | water model | ice Ih | liquid |
| 220 | TIP4P | 15.850 | 15.811 |
| 225 | TIP4P | 15.941 | 15.918 |
| 230 | TIP4P | 16.040 | 16.034 |
| 235 | TIP4P | 16.135 | 16.136 |
| 240 | TIP4P | 16.229 | 16.267 |
| 253 | WAIL | −16.218 | −16.099 |
| 273 | WAIL | −16.391 | −16.391 |
| 293 | WAIL | −16.621 | −16.767 |

Jarzynski's estimator[12] over 20 repetitions for TIP4P and 10 repetitions for WAIL. The error bars were determined with bootstrap resampling with replacement.[68] For solid simulations, Jarzynski's estimator was applied independently to each step. As discussed previously, because each realization of the liquid to Einstein crystal transformation goes through a different glassy state, the Jarzynski estimator was applied only to the sum of the liquid steps. A detailed report of the procedure for the melting free energy calculation including the integrated work of each repetition is reported in the Supporting Information for TIP4P at 240 K to serve as an example.

The $\Delta G_{melting}$ for TIP4P is plotted in Figure 3a. A negative $\Delta G_{melting}$ indicates that the liquid phase is more stable. A linear least-square fit to the data indicates that the TIP4P model has a $T_M$ of 232 ± 1 K. The $T_M$ of ice Ih for the TIP4P model has been studied extensively. For example, Fernandez et al.[34] estimated it to be 230 ± 3 K; Bai et al.[34] and Koyama et al.[33] independently determined it to be around 229 K, and the Vega group[34,38,59] reported it to be 232 ± 5 K. The 232 ± 1 K $T_M$ in this work is in close agreement with these studies.

In our work, different proton configurations were sampled, with the electrostatic switching method published previously.[40,57] Thus, the Pauling entropy[69] is not added to our solid-state free energy.

The excess free energies for the solid and liquid of the WAIL water are also reported in Table 4 and plotted in Figure 3b. A linear least-squares regression gives a $T_M$ of 272 ± 1 K. This is consistent with the previously reported value of 271 K.[40] As



DOI: 10.1021/acs.jpcb.9b06840
J. Phys. Chem. B 2019, 123, 7740−7747

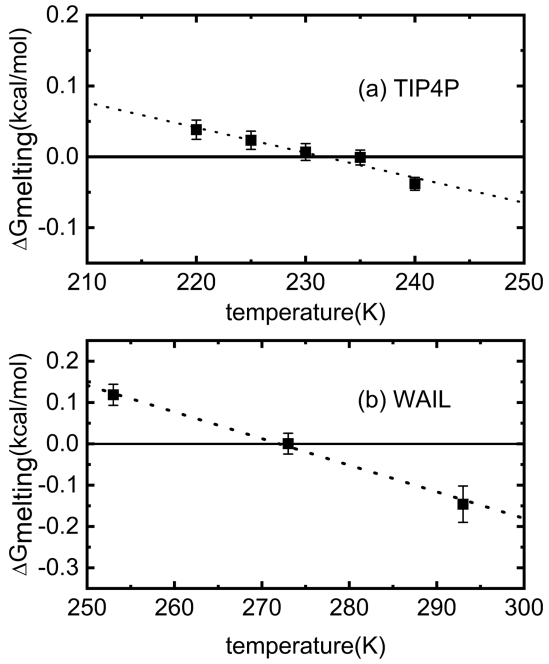


**Figure 3.** Gibbs free energy of melting for TIP4P (a) and WAIL (b) water models as a function of temperature. A positive value indicates that ice Ih is more stable. The dotted line is the linear least-squares fit used to interpolate the melting temperature.

reported previously,[40] the WAIL potential also correctly reproduces the radial distribution functions of both ice Ih and liquid water. Additionally, it produces a temperature of maximum density of 9 °C and predicts the correct heat of vaporization after quantum nuclear effects are properly modeled with path-integral molecular dynamics.[40]

The entropy of melting can be obtained by measuring the slopes in Figure 3. The TIP4P entropy of melting is 3.54 ± 0.47 cal/mol·K, in reasonable agreement with the value of 4.56 cal/mol·K reported previously by Vega et al.[70] The WAIL entropy of melting is 6.44 ± 1.19 cal/mol·K, overestimating the experimental value of 5.25 cal/mol·K.[71] This overestimation is consistent with the missing quantum nuclear effect in this study based on classical molecular dynamics.[72] The experimental entropy of melting of $D_2O$ is about 0.2 cal/mol·K higher than that of $H_2O$.[73,74] The entropy of melting is a thermodynamic property that should not depend on the isotope mass within classical statistical mechanics; the observed difference in entropy of melting for heavy water indicates that accounting for nuclear quantum effects should have a negative contribution to the entropy. Thus, a classical simulation should overestimate the experimental entropy of melting when a Born−Oppenheimer model potential is being used.

In order to perform an independent verification of the WAIL $T_M$, simulations of an ice slab in liquid water was performed following the direct coexistence method.[34,36,45,75] The initial configuration contained 7 layers of ice and 300 liquid molecules. The system was kept at 1 atm at a series of temperatures close to 272 K. The temperature and pressure were maintained with the Nosé−Hoover thermostat and the anisotropic Parrinello−Rahman barostat, respectively. A thermostat relaxation time of 0.2 ps and a barostat relaxation time of 2 ps were used. The potential energy of the ice−water coexistence at 270 and 271 K is reported as a function of time in Figure 4. The potential energy increased with time at 271 K, indicating gradual melting of ice, which is exothermic. At 270 K, the potential energy decreased, consistent with gradual growth of ice. This observation is in good agreement with the prediction of our free energy study.

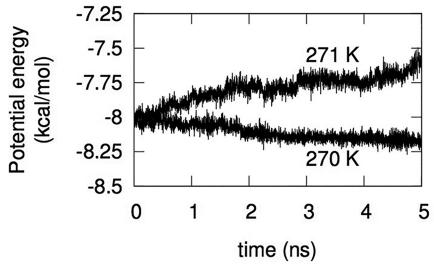


**Figure 4.** Potential energy for an ice−water interface with 591 water molecules described by the WAIL potential reported as a function of time at 270 and 271 K.

## 5. SUMMARY

In this work, the glassy intermediate scheme is shown to be capable of measuring the excess free energy of liquid water relative to an Einstein crystal without going through a first-order phase transition. This is accomplished by taking advantage of the fact that vitrification of a liquid occurs without a singularity in response functions. Although the free energy of glass is not well-defined, a "free energy" can be evaluated for each glassy intermediate state. Such an intermediate state is used to complete the thermodynamic path for the transformation from a liquid to an Einstein crystal. Because the "free energy" of the intermediate state cancels, the excess free energy relative to the Einstein crystal is insensitive to the choice of the intermediate state. Going through such glassy intermediate states allows the excess free energy of a liquid to be determined without integrating over a singularity. Combined with the excess free energy of the solid, we demonstrated a protocol to determine the melting free energy of ice. In our procedure, once the tethering points have been determined, all remaining steps can be performed in parallel.

Considering the large overlap of configuration space between liquid and glassy water and similarly between the intermediate and Einstein crystal tethered to the glassy configuration, the glassy intermediate approach follows a highly efficient thermodynamic path. The thermodynamic path was tested for the determination of $T_M$ for both the TIP4P and WAIL water potentials. The $T_M$ of TIP4P was determined to be 232 ± 1 K, which is in good agreement with literature values. The $T_M$ of WAIL water was determined to be 272 ± 1 K and agrees well with that of real water. Additionally, the $T_M$ of WAIL is corroborated with direct coexistence simulations, which give $T_M$ values between 270 to 271 K. Considering that no experimental data was fit to develop the WAIL potential, the good prediction of $T_M$ is encouraging validation of the quality of such an electronic structure based potential.[40]

Although vitrification of liquid water is challenging experimentally, liquid water can be easily vitrified in a simulation. Admittedly our method may not be applicable to materials that undergo rapid crystallization even on a nanosecond time scale during a simulation. However, for many materials, where vitrification can be achieved, our glassy


DOI: 10.1021/acs.jpcb.9b06840
J. Phys. Chem. B 2019, 123, 7740−7747

intermediate method can be used to calculate the excess free energy of the liquid.

## ■ ASSOCIATED CONTENT

### Supporting Information

The Supporting Information is available free of charge on the ACS Publications website at DOI: 10.1021/acs.jpcb.9b06840.

Calculation example for the determination of the free energy of melting for TIP4P ice at 240 K and another measure of the melting temperature of TIP4P ice, where the switching rates for the vitrification step and the first tethering step were changed (PDF)

## ■ AUTHOR INFORMATION


### Corresponding Author

*E-mail: fengwang@uark.edu.

### ORCID

Gerrick E. Lindberg: 0000-0002-5292-4200

Xin-Zheng Li: 0000-0003-0316-4257

Feng Wang: 0000-0002-2740-3534


### Notes

The authors declare no competing financial interest.

## ■ ACKNOWLEDGMENTS

This work was supported by NSF Award DMR-1609650 and by the Arkansas Biosciences Institute. The computer resources for this study were provided by the Arkansas High Performance Computational Center supported by NSF MRI-R2 0959124.

## ■ REFERENCES


(1) Angell, C. A. Supercooled Water. *Annu. Rev. Phys. Chem.* **1983**, *34*, 593−630.

(2) Goncharov, A. F.; Goldman, N.; Fried, L. E.; Crowhurst, J. C.; Kuo, I-F. W.; Mundy, C. J.; Zaug, J. M. Dynamic Ionization of Water under Extreme Conditions. *Phys. Rev. Lett.* **2005**, *94*, 125508.

(3) Eike, D. M.; Maginn, E. J. Atomistic Simulation of Solid-Liquid Coexistence for Molecular Systems: Application to Triazole and Benzene. *J. Chem. Phys.* **2006**, *124*, 164503.

(4) Grochola, G. Constrained Fluid Λ-Integration: Constructing a Reversible Thermodynamic Path between the Solid and Liquid State. *J. Chem. Phys.* **2004**, *120*, 2122−2126.

(5) Eike, D. M.; Brennecke, J. F.; Maginn, E. J. Toward a Robust and General Molecular Simulation Method for Computing Solid-Liquid Coexistence. *J. Chem. Phys.* **2005**, *122*, 014115.

(6) Vega, C.; Abascal, J. L. F. Simulating Water with Rigid Non-Polarizable Models: A General Perspective. *Phys. Chem. Chem. Phys.* **2011**, *13*, 19663−19688.

(7) Warshel, A.; Kato, M.; Pisliakov, A. V. Polarizable Force Fields: History, Test Cases, and Prospects. *J. Chem. Theory Comput.* **2007**, *3*, 2034−2045.

(8) Frenkel, D.; Ladd, A. J. C. New Monte Carlo Method to Compute the Free Energy of Arbitrary Solids. Application to the fcc and hcp Phases of Hard Spheres. *J. Chem. Phys.* **1984**, *81*, 3188−3193.

(9) de Koning, M.; Antonelli, A. Einstein Crystal as a Reference System in Free Energy Estimation Using Adiabatic Switching. *Phys. Rev. E: Stat. Phys., Plasmas, Fluids, Relat. Interdiscip. Top.* **1996**, *53*, 465−474.

(10) Kirkwood, J. G. Statistical Mechanics of Fluid Mixtures. *J. Chem. Phys.* **1935**, *3*, 300−313.

(11) Bennett, C. Efficient Estimation of Free Energy Differences from Monte Carlo Data. *J. Comput. Phys.* **1976**, *22*, 245−268.

(12) Jarzynski, C. Nonequilibrium Equality for Free Energy Differences. *Phys. Rev. Lett.* **1997**, *78*, 2690−2693.

(13) Jarzynski, C. Equilibrium Free-Energy Differences from Nonequilibrium Measurements: A Master-Equation Approach. *Phys. Rev. E: Stat. Phys., Plasmas, Fluids, Relat. Interdiscip. Top.* **1997**, *56*, 5018−5035.

(14) Noya, E.; Conde, M.; Vega, C. Computing the Free Energy of Molecular Solids by the Einstein Molecule Approach: Ices XIII and XIV, Hard-Dumbbells and a Patchy Model of Proteins. *J. Chem. Phys.* **2008**, *129*, 104704.

(15) Habershon, S.; Manolopoulos, D. Free Energy Calculations for a Flexible Water Model. *Phys. Chem. Chem. Phys.* **2011**, *13*, 19714−19727.

(16) Gao, G. T.; Zeng, X. C.; Tanaka, H. The Melting Temperature of Proton-Disordered Hexagonal Ice: A Computer Simulation of 4-Site Transferable Intermolecular Potential Model of Water. *J. Chem. Phys.* **2000**, *112*, 8534−8538.

(17) Vega, C.; Noya, E. Revisiting the Frenkel-Ladd Method to Compute the Free Energy of Solids: The Einstein Molecule Approach. *J. Chem. Phys.* **2007**, *127*, 154113.

(18) Aragones, J.; Noya, E.; Valeriani, C.; Vega, C. Free Energy Calculations for Molecular Solids Using Gromacs. *J. Chem. Phys.* **2013**, *139*, 034104.

(19) Navascués, G.; Velasco, E. Efficient Approach to the Free Energy of Crystals Via Monte Carlo Simulations: Application to Continuous and Orientation-Dependent Potentials. *Phys. Rev. E: Stat. Phys., Plasmas, Fluids, Relat. Interdiscip. Top.* **2017**, *95*, 032140.

(20) Reddy A, R. K.; Punnathanam, S. Calculation of Excess Free Energy of Molecular Solids Comprised of Flexible Molecules Using Einstein Molecule Method. *Mol. Simul.* **2018**, *44*, 781−788.

(21) Moustafa, S. G.; Schultz, A. J.; Kofke, D. A. Harmonically Assisted Methods for Computing the Free Energy of Classical Crystals by Molecular Simulation: A Comparative Study. *J. Chem. Theory Comput.* **2017**, *13*, 825−834.

(22) Widom, B. Some Topics in the Theory of Fluids. *J. Chem. Phys.* **1963**, *39*, 2808−2812.

(23) Vlot, M. J.; Huinink, J.; van der Eerden, J. P. Free Energy Calculations on Systems of Rigid Molecules: An Application to the Tip4p Model of $H_2O$. *J. Chem. Phys.* **1999**, *110*, 55−61.

(24) Panagiotopoulos, A. Direct Determination of Phase Coexistence Properties of Fluids by Monte-Carlo Simulation in a New Ensemble. *Mol. Phys.* **1987**, *61*, 813−826.

(25) Heidari, M.; Kremer, K.; Cortes-Huerto, R.; Potestio, R. Spatially Resolved Thermodynamic Integration: An Efficient Method to Compute Chemical Potentials of Dense Fluids. *J. Chem. Theory Comput.* **2018**, *14*, 3409−3417.

(26) Shing, K. S.; Gubbins, K. E. The Chemical Potential in Dense Fluids and Fluid Mixtures Via Computer Simulation. *Mol. Phys.* **1982**, *46*, 1109−1128.

(27) Shing, K. S.; Gubbins, K. E. The Chemical Potential in Non-Ideal Liquid Mixtures. *Mol. Phys.* **1983**, *49*, 1121−1138.

(28) Kauzmann, W. The Nature of the Glassy State and the Behavior of Liquids at Low Temperature. *Chem. Rev.* **1948**, *43*, 219−256.

(29) Schilling, T.; Schmid, F. Computing Absolute Free Energies of Disordered Structures by Molecular Simulation. *J. Chem. Phys.* **2009**, *131*, 231102.

(30) Schmid, F.; Schilling, T. A Method to Compute Absolute Free Energies or Enthalpies of Fluids. *Phys. Procedia* **2010**, *4*, 131−143.

(31) Kroes, G.-J. Surface Melting of the (0001) Face of Tip4p Ice. *Surf. Sci.* **1992**, *275*, 365−382.

(32) Nada, H.; van der Eerden, J. P. J. M. An Intermolecular Potential Model for the Simulation of Ice and Water near the Melting Point: A Six-Site Model of $H_2O$. *J. Chem. Phys.* **2003**, *118*, 7401−7413.

(33) Koyama, Y.; Tanaka, H.; Gao, G.; Zeng, X. C. Melting Points and Thermal Expansivities of Proton-Disordered Hexagonal Ice with Several Model Potentials. *J. Chem. Phys.* **2004**, *121*, 7926−7931.

(34) García Fernández, R.; Abascal, J. L. F.; Vega, C. The Melting Point of Ice Ih for Common Water Models Calculated from Direct Coexistence of the Solid-Liquid Interface. *J. Chem. Phys.* **2006**, *124*, 144506.

(35) Sanz, E.; Vega, C.; Abascal, J. L. F.; MacDowell, L. Phase Diagram of Water from Computer Simulation. *Phys. Rev. Lett.* **2004**, *92*, 255701.
(36) Karim, O.; Haymet, A. The Ice/Water Interface. *Chem. Phys. Lett.* **1987**, *138*, 531−534.
(37) Handel, R.; Davidchack, R.; Anwar, J.; Brukhno, A. Direct Calculation of Solid-Liquid Interfacial Free Energy for Molecular Systems: Tip4p Ice-Water Interface. *Phys. Rev. Lett.* **2008**, *100*, 036104.
(38) Vega, C.; Martin-Conde, M.; Patrykiejew, A. Absence of Superheating for Ice Ih with a Free Surface: A New Method of Determining the Melting Point of Different Water Models. *Mol. Phys.* **2006**, *104*, 3583−3592.
(39) Báez, L. A.; Clancy, P. Phase Equilibria in Extended Simple Point Charge Ice-Water Systems. *J. Chem. Phys.* **1995**, *103*, 9744−9755.
(40) Pinnick, E. R.; Erramilli, S.; Wang, F. Predicting the Melting Temperature of Ice-Ih with Only Electronic Structure Information as Input. *J. Chem. Phys.* **2012**, *137*, 014510.
(41) Akin-Ojo, O.; Song, Y.; Wang, F. Developing ab initio Quality Force Fields from Condensed Phase Quantum-Mechanics/Molecular-Mechanics Calculations through the Adaptive Force Matching Method. *J. Chem. Phys.* **2008**, *129*, 064108.
(42) Akin-Ojo, O.; Wang, F. Improving the Point-Charge Description of Hydrogen Bonds by Adaptive Force Matching. *J. Phys. Chem. B* **2009**, *113*, 1237−1240.
(43) Akin-Ojo, O.; Wang, F. The Quest for the Best Nonpolarizable Water Model from the Adaptive Force Matching Method. *J. Comput. Chem.* **2011**, *32*, 453−462.
(44) Wang, F.; Akin-Ojo, O.; Pinnick, E.; Song, Y. Approaching Post-Hartree-Fock Quality Potential Energy Surfaces with Simple Pair-Wise Expressions: Parameterising Point-Charge-Based Force Fields for Liquid Water Using the Adaptive Force Matching Method. *Mol. Simul.* **2011**, *37*, 591−605.
(45) Ladd, A. J. C.; Woodcock, L. Triple-Point Coexistence Properties of the Lennard-Jones System. *Chem. Phys. Lett.* **1977**, *51*, 155−159.
(46) Ladd, A. J. C.; Woodcock, L. Interfacial and Co-Existence Properties of the Lennard-Jones System at the Triple Point. *Mol. Phys.* **1978**, *36*, 611−619.
(47) Cape, J. N.; Woodcock, L. V. Molecular Dynamics Calculation of Phase Coexistence Properties: The Soft-Sphere Melting Transition. *Chem. Phys. Lett.* **1978**, *59*, 271−274.
(48) Zwanzig, R. W. High-Temperature Equation of State by a Perturbation Method. I. Nonpolar Gases. *J. Chem. Phys.* **1954**, *22*, 1420−1426.
(49) Hermans, J. Simple Analysis of Noise and Hysteresis in (Slow-Growth) Free Energy Simulations. *J. Phys. Chem.* **1991**, *95*, 9029−9032.
(50) Kästner, J.; Thiel, W. Bridging the Gap between Thermodynamic Integration and Umbrella Sampling Provides a Novel Analysis Method: "Umbrella Integration. *J. Chem. Phys.* **2005**, *123*, 144104.
(51) Beveridge, D. L.; Dicapua, F. M. Free Energy Via Molecular Simulation: Applications to Chemical and Biomolecular Systems. *Annu. Rev. Biophys. Biophys. Chem.* **1989**, *18*, 431−492.
(52) Laio, A.; Parrinello, M. Escaping Free-Energy Minima. *Proc. Natl. Acad. Sci. U. S. A.* **2002**, *99*, 12562−12566.
(53) To obtain a copy of the inhouse DLPOLY code, please contact the corresponding author.
(54) Smith, W.; Forester, T. R. Dl_Poly_2.0: A General-Purpose Parallel Molecular Dynamics Simulation Package. *J. Mol. Graphics* **1996**, *14*, 136−141.
(55) Todorov, I. T.; Smith, W.; Trachenko, K.; Dove, M. T. Dl_Poly_3: New Dimensions in Molecular Dynamics Simulations Via Massive Parallelism. *J. Mater. Chem.* **2006**, *16*, 1911−1918.
(56) Beutler, T. C.; Mark, A. E.; van Schaik, R. C.; Gerber, P. R.; van Gunsteren, W. F. Avoiding Singularities and Numerical Instabilities in Free Energy Calculations Based on Molecular Simulations. *Chem. Phys. Lett.* **1994**, *222*, 529−539.
(57) Lindberg, G.; Wang, F. Efficient Sampling of Ice Structures by Electrostatic Switching. *J. Phys. Chem. B* **2008**, *112*, 6436−6441.
(58) Vega, C.; Abascal, J. L. F.; Sanz, E.; MacDowell, L.; McBride, C. Can Simple Models Describe the Phase Diagram of Water? *J. Phys.: Condens. Matter* **2005**, *17*, S3283−S3288.
(59) Vega, C.; Sanz, E.; Abascal, J. L. F. The Melting Temperature of the Most Common Models of Water. *J. Chem. Phys.* **2005**, *122*, 114507.
(60) Martyna, G. J.; Klein, M. L.; Tuckerman, M. Nosé-Hoover Chains: The Canonical Ensemble Via Continuous Dynamics. *J. Chem. Phys.* **1992**, *97*, 2635−2643.
(61) Essmann, U.; Perera, L.; Berkowitz, M. L.; Darden, T.; Lee, H.; Pedersen, L. G. A Smooth Particle Mesh Ewald Method. *J. Chem. Phys.* **1995**, *103*, 8577−8593.
(62) Melchionna, S.; Ciccotti, G.; Holian, B. L. Hoover Npt Dynamics for Systems Varying in Shape and Size. *Mol. Phys.* **1993**, *78*, 533−544.
(63) Abascal, J. L. F.; Sanz, E.; García Fernández, R.; Vega, C. A Potential Model for the Study of Ices and Amorphous Water: Tip4p/Ice. *J. Chem. Phys.* **2005**, *122*, 234511.
(64) Allen, M. P.; Tildesley, D. J. *Computer Simulation of Liquids*; Oxford University Press: New York, 1987.
(65) Lindberg, G. E.; Berkelbach, T. C.; Wang, F. Optimizing the Switching Function for Nonequilibrium Free-Energy Calculations: An on-the-Fly Approach. *J. Chem. Phys.* **2009**, *130*, 174705.
(66) Anwar, J.; Heyes, D. M. Robust and Accurate Method for Free-Energy Calculation of Charged Molecular Systems. *J. Chem. Phys.* **2005**, *122*, 224117.
(67) Kob, W.; Andersen, H. C. Testing Mode-Coupling Theory for a Supercooled Binary Lennard-Jones Mixture I: The Van Hove Correlation Function. *Phys. Rev. E: Stat. Phys., Plasmas, Fluids, Relat. Interdiscip. Top.* **1995**, *51*, 4626−4641.
(68) Efron, B. Bootstrap Methods: Another Look at the Jackknife. *Ann. Statist* **1979**, *7*, 1−26.
(69) Pauling, L. The Structure and Entropy of Ice and of Other Crystals with Some Randomness of Atomic Arrangement. *J. Am. Chem. Soc.* **1935**, *57*, 2680−2684.
(70) Espinosa, J. R.; Vega, C.; Sanz, E. Ice-Water Interfacial Free Energy for the TIP4P, TIP4P/2005, TIP4P/Ice, and mW Models as Obtained from the Mold Integration Technique. *J. Phys. Chem. C* **2016**, *120*, 8068−8075.
(71) Eisenberg, D.; Kauzmann, W. *The Structure and Properties of Water*; Oxford University Press: New York, 1969.
(72) Ramirez, R.; Herrero, C. P. Quantum Path Integral Simulation of Isotope Effects in the Melting Temperature of Ice Ih. *J. Chem. Phys.* **2010**, *133*, 144511.
(73) McBride, C.; Aragones, J. L.; Noya, E. G.; Vega, C. A Study of the Influence of Isotopic Substitution on the Melting Point and Temperature of Maximum Density of Water by Means of Path Integral Simulations of Rigid Models. *Phys. Chem. Chem. Phys.* **2012**, *14*, 15199−15205.
(74) Wagner, W.; Pruß, A. The Iapws Formulation 1995 for the Thermodynamic Properties of Ordinary Water Substance for General and Scientific Use. *J. Phys. Chem. Ref. Data* **2002**, *31*, 387−535.
(75) Conde, M. M.; Rovere, M.; Gallo, P. High Precision Determination of the Melting Points of Water TIP4P/2005 and Water TIP4P/Ice Models by the Direct Coexistence Technique. *J. Chem. Phys.* **2017**, *147*, 244506.


DOI: 10.1021/acs.jpcb.9b06840
*J. Phys. Chem. B* 2019, 123, 7740−7747